Immunity
Article

Bcl6 Protein Expression Shapes Pre-Germinal Center B Cell Dynamics and Follicular Helper T Cell Heterogeneity

Masahiro Kitano,[1,6] Saya Moriyama,[2,3,6] Yoshikazu Ando,[1] Masaki Hikida,[2,7] Yasuo Mori,[4] Tomohiro Kurosaki,[2,3,5] and Takaharu Okada[1,4,*]
[1]Research Unit for Immunodynamics
[2]Laboratory for Lymphocyte Differentiation
RIKEN, Research Center for Allergy and Immunology, Yokohama, 230-0045, Japan
[3]Graduate School of Frontier Biosciences, Osaka University, Suita, Osaka 565-0871, Japan
[4]Innovative Techno-Hub for Integrated Medical Bio-imaging, Department of Synthetic Chemistry and Biological Chemistry, Graduate School of Engineering, Kyoto University, Kyoto, 615-8530, Japan
[5]WPI Immunology Frontier Research Center, Osaka University, Suita, 565-0871, Japan
[6]These authors contributed equally to this work
[7]Present address: Center for Innovation in Immunoregulative Technology and Therapeutics, Graduate School of Medicine, Kyoto University, Kyoto, 606-8501, Japan
*Correspondence: tokada@rcai.riken.jp
DOI 10.1016/j.immuni.2011.03.025

SUMMARY

The transcription factor Bcl6 is essential for the development of germinal center (GC) B cells and follicular helper T (Tfh) cells. However, little is known about in vivo dynamics of Bcl6 protein expression during and after development of these cells. By using a Bcl6 reporter mouse strain, we found that antigen-engaged B cells upregulated Bcl6 before clustering in GCs. Two-photon microscopic analysis indicated that Bcl6 upregulation in pre-GC B cells contributed to sustaining their interactions with helper T cells and was required for their entry to GC clusters. Our data also suggested that Tfh cells gradually downmodulated Bcl6 protein over weeks after development. The Bcl6-low Tfh cells rapidly terminated proliferation and upregulated IL-7 receptor. These results clarify the role of Bcl6 in pre-GC B cell dynamics and highlight the modulation of Bcl6 expression in Tfh cells that persist in the late phase of the antibody response.

INTRODUCTION

The germinal center (GC) is the important microstructure formed in the B cell follicle of the secondary lymphoid organs for producing long-term, high-affinity antibody (Ab) responses (MacLennan, 1994). In most Ab responses against protein antigens (Ags), GC B cells, which are characterized by the $GL7^{hi}$, Fas^{hi}, $CD38^{lo}$ (in mice), and IgD^{lo} surface phenotype, are dependent on help provided by $CD4^+$ T cells for their development, maintenance, and possibly the selection (Allen et al., 2007a; Kurosaki et al., 2010; Victora et al., 2010; Vinuesa et al., 2010). Helper T cells residing in the B cell follicles and GCs are named follicular helper T (Tfh) cells and highly express surface molecules including CXCR5 and PD-1 and the cytokines IL-21 and IL-4 (Allen et al., 2007a; Good-Jacobson et al., 2010; Vinuesa et al., 2010). The generation of Tfh cells usually requires interactions of $CD4^+$ T cells with cognate Ag-engaged B cells, dynamics of which is featured by sustained conjugation of these cells, and in turn, is essential for GC B cell development and/or maintenance (Crotty et al., 2010; Linterman and Vinuesa, 2010).

The transcription factor Bcl6 was discovered to be essential for the GC formation more than a decade ago (Dent et al., 1997; Fukuda et al., 1997; Ye et al., 1997). Bcl6 protein is abundantly expressed in GC B cells compared to naive B cells, and B cells intrinsically require Bcl6 for their development into GC B cells (Crotty et al., 2010; Klein and Dalla-Favera, 2008; Nurieva et al., 2009; Shaffer et al., 2001; Yu et al., 2009). Bcl6 can repress a number of target genes and has various functions in GC B cell biology including protection from DNA damage-induced apoptosis and inhibition of differentiation to plasma cells or memory cells (Klein and Dalla-Favera, 2008). Bcl6 expression also modulates costimulatory signals relevant in interactions with helper T cells (Klein and Dalla-Favera, 2008). However, it is not known whether Bcl6 expression can modulate B cell-T cell interaction dynamics. In addition, Bcl6 has been suggested to be important for the GC B cell localization. Bcl6 represses expression of *Gpr183*, encoding a G protein-coupled receptor EBI-2 (Shaffer et al., 2001). Upregulation and downregulation of EBI-2 have been shown to be important for the localization of Ag-engaged B cells in the outer follicle region and subsequent clustering of GC B cells in the inner region of the follicle, respectively (Gatto et al., 2009; Pereira et al., 2009). Thus, it has been suggested that Bcl6 controls GC B cell positioning via this pathway (Chan et al., 2010; Pereira et al., 2010). However, whether Bcl6 upregulation in B cells begins in the outer follicle to drive them to cluster in GCs or it occurs in B cells that have briefly accessed the inner follicle to retain them in the region remains to be clarified.

Recently, Tfh cell development was also found to be strictly dependent on Bcl6 (Johnston et al., 2009; Nurieva et al., 2009; Yu et al., 2009). $CD4^+$ T cells modestly upregulate *Bcl6*

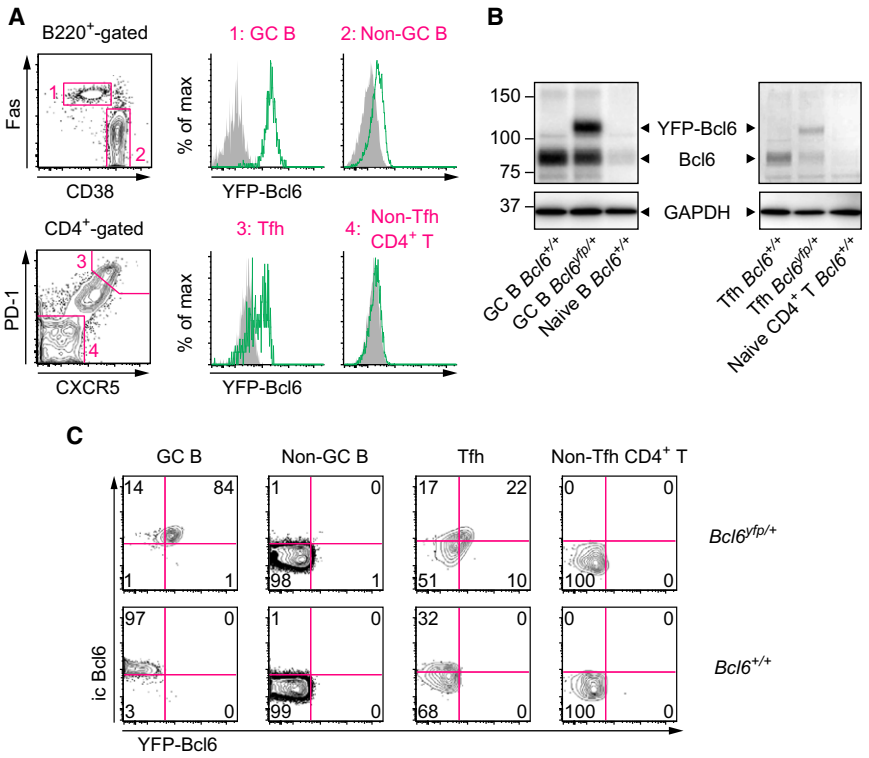

Figure 1. Characterization of *Bcl6*^{yfp} Mice

(A) Flow cytometry of PP cells from *Bcl6*$^{yfp/+}$ mice. Shaded histograms show *Bcl6*$^{+/+}$ control cells.

(B) Immunoblot analysis of Bcl6 and YFP-Bcl6 protein expression in GC B cells, naive B cells, Tfh cells, and naive CD4$^+$ T cells of the indicated genotypes.

(C) Intracellular Bcl6 staining signals (ic Bcl6) in PP cells from *Bcl6*$^{yfp/+}$ mice and *Bcl6*$^{+/+}$ mice were analyzed. Note that YFP-Bcl6 fluorescence was slightly reduced by cell fixation. The numbers show the percentages of cells in the gates.

transcripts through interactions with non-B cell Ag-presenting cells, presumably dendritic cells (Poholek et al., 2010). CD4$^+$ T cells further upregulate *Bcl6* expression through sustained cognate interactions with B cells, which is important for Tfh cell development (Crotty et al., 2010; Deenick et al., 2010; Linterman and Vinuesa, 2010; Poholek et al., 2010). Although expression of *Bcl6* transcripts in CD4$^+$ T cells has been analyzed in the various settings of immune responses, dynamics of Bcl6 protein expression during the Tfh cell development still need to be understood because *Bcl6* mRNA quantities are in some cases a poor indicator of Bcl6 protein expression (Crotty et al., 2010; Klein and Dalla-Favera, 2008). Moreover, little is known about the stability of Bcl6 expression in Tfh cells after their development despite its potential importance in their fate decision.

In order to understand Bcl6 expression dynamics in B cells and helper T cells during the Ab response and to address the questions raised above, we developed a reporter mouse strain to track Bcl6 protein expression in vivo. By utilizing the reporter mouse we provide evidence that Bcl6 upregulation of B cells in the outer follicle sustains their interactions with helper T cells and allows them to enter the GC region. Our results also highlight the Tfh cell heterogeneity in Bcl6 protein expression and suggest that tuning of Bcl6 expression is linked to the regulation of Tfh cell proliferation and gene expression pertaining to their homeostatic cytokine responsiveness and migration potential.

RESULTS

Generation and Characterization of the *Bcl6*^{yfp} Mice

To analyze Bcl6 protein expression in vivo, we generated a reporter mouse strain by gene targeting. The monomeric yellow fluorescent protein (YFP) gene was inserted in-frame right after the initiation codon of the *Bcl6* gene such that the product of this allele would be the YFP-Bcl6 fusion protein (Figure S1A available online). Flow cytometric analysis of Peyer's patch (PP) cells from heterozygous mice detected substantial YFP signals in more than 90% of GC B cells and weak YFP signals in non-GC B cells (Figure 1A). Within CD4$^+$ T cells, YFP signals were selectively found in the CXCR5^{hi}PD-1^{hi} Tfh cell population although these cells appeared to be more heterogeneous in YFP expression than GC B cells (Figure 1A). Even Tfh cells with the highest CXCR5 and PD-1 expression were found to be heterogeneous in YFP-Bcl6 expression (Figure S1B). Immunoblot analysis of sorted *Bcl6*$^{+/+}$ GC B cells with anti-Bcl6 detected a protein of the Bcl6 size (79 kDa), which appeared to be far more abundant in GC B cells than in naive B cells (Figure 1B) and was undetectable in *Bcl6*$^{yfp/yfp}$ naive B cells (Figure S1C). In addition to this protein, the Ab detected another protein of the YFP-Bcl6 size (107 kDa) in *Bcl6*$^{yfp/+}$ GC B cells, but not in *Bcl6*$^{+/+}$ GC B cells. Importantly, heterozygous cells expressed similar amounts of these two anti-Bcl6-reactive proteins given that the YFP-Bcl6 band intensity was 115% ± 7.52% for *Bcl6*$^{yfp/+}$ B cells (mean ± SEM, n = 3) and 103% ± 17.7% for *Bcl6*$^{yfp/+}$ Tfh cells (n = 4) of the Bcl6 band intensity. The amount of Bcl6 produced by the wild-type allele of heterozygous cells was 69.6% ± 9.25% (*Bcl6*$^{yfp/+}$ B cells, n = 3) and 62.5% ± 19.6% (*Bcl6*$^{yfp/+}$ Tfh cells, n = 4) of the Bcl6 amount in wild-type B cells and Tfh cells, respectively. We also performed intracellular staining with anti-Bcl6 for flow cytometry, and found that the YFP signals were well correlated with the intracellular staining signals both in GC B cells and Tfh cells (Figure 1C). Thus, the YFP signal derived from the *Bcl6*^{yfp} allele of heterozygous mice serves as a reliable reporter for Bcl6 protein expression.

Whereas GC B cells and Tfh cells in *Bcl6*$^{yfp/+}$ mice were not significantly decreased compared to wild-type mice, *Bcl6*$^{yfp/yfp}$ mice had reduced numbers of GC B cells and Tfh cells in PPs (Figure S1D). These results indicate that YFP fusion near the N terminus compromised Bcl6 function, although *Bcl6*$^{yfp/yfp}$ mice are healthy unlike Bcl6-deficient mice (Dent et al., 1997; Fukuda et al., 1997; Ye et al., 1997). However, serum immunoglobulin titers of the isotypes tested were not significantly altered in

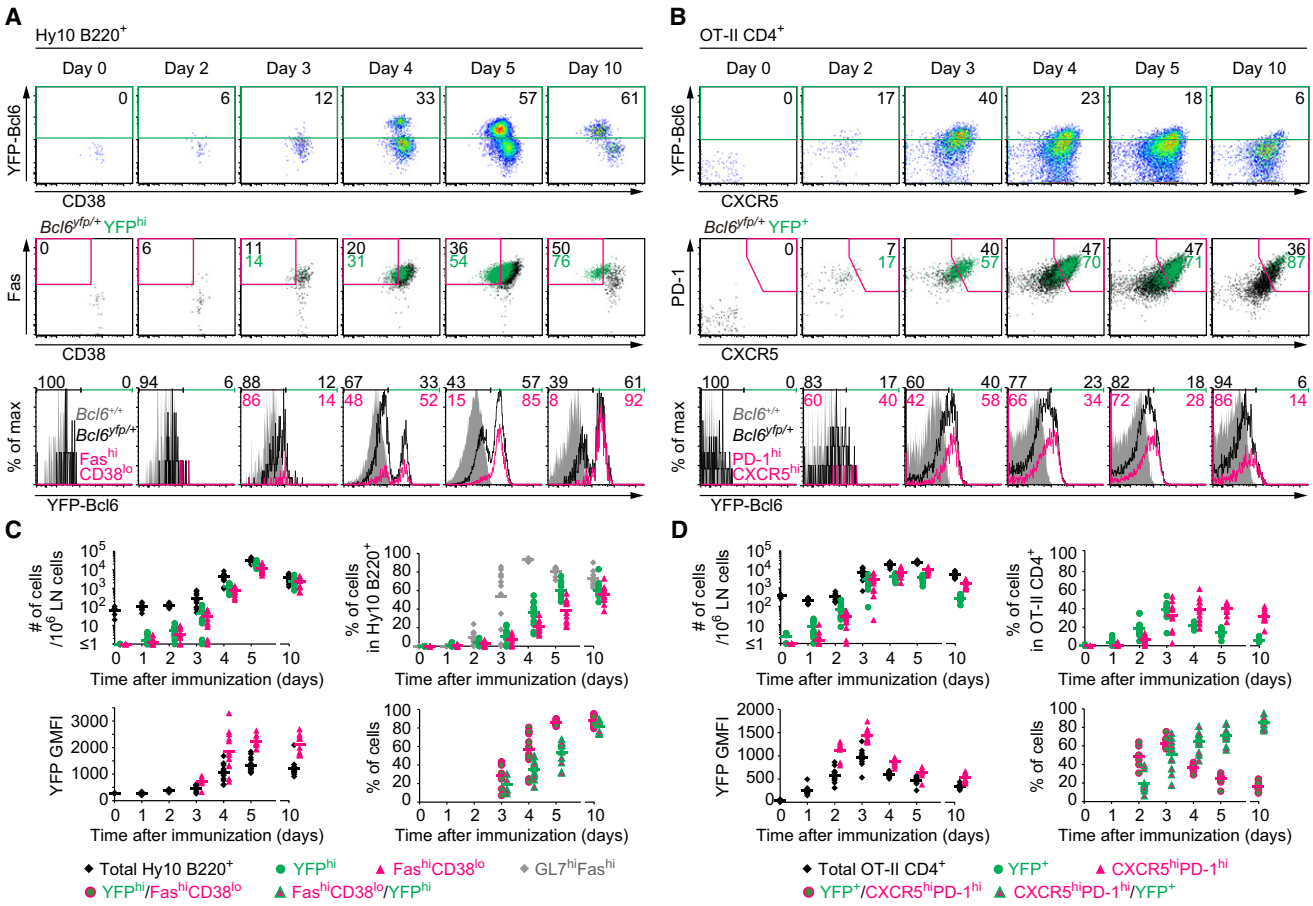

Figure 2. Kinetics of YFP-Bcl6 Expression in Ag-Engaged B Cells and Helper T Cells

(A and B) Representative flow cytometry plots of adoptively transferred *Bcl6*$^{yfp/+}$ Hy10 B cells (A) and *Bcl6*$^{yfp/+}$ OT-II T cells (B) in draining LNs after immunization with HEL-OVA in CFA. In the middle row, YFP^{hi} Hy10 B cells and YFP^{+} OT-II T cells (gated in the top row) were shown as green dots. In the bottom row, histograms show YFP-Bcl6 expression in total *Bcl6*$^{yfp/+}$ Hy10 B cells, Fas^{hi}CD38^{lo} Hy10 B cells (gated in the middle row), total *Bcl6*$^{yfp/+}$ OT-II T cells, and CXCR5^{hi}PD-1^{hi} OT-II T cells (gated in the middle row).

(C and D) Enumeration of the *Bcl6*$^{yfp/+}$ Hy10 B cell populations (C) and the *Bcl6*$^{yfp/+}$ OT-II T cell populations (D). The symbol color corresponds to the gate color in (A) and (B). The percentages were calculated from data containing at least 10 cells for the denominator. Each symbol object represents a data of a LN, and bars show averaged values. Data are of six LNs (day 0) and 12 LNs (days 2–10) from three mice for each time point in two independent experiments. GMFI, geometric mean fluorescent intensity.

Bcl6$^{yfp/+}$ mice or *Bcl6*$^{yfp/yfp}$ mice, suggesting that Ab class-switching is not affected by the *Bcl6*^{yfp} allele (Figure S1E).

Kinetics of Bcl6 Protein Expression in Ag-Engaged B Cells and CD4^{+} T Cells

To track Bcl6 expression in Ag-engaged B cells and CD4^{+} T cells, we crossed *Bcl6*^{yfp} mice to avian lysozyme-specific Hy10 (aka VDJ9/κ5) B cell receptor (BCR) gene-targeted transgenic mice (Allen et al., 2007b) or to OT-II T cell receptor (TCR) transgenic mice. *Bcl6*$^{yfp/+}$ Hy10 B cells and *Bcl6*$^{yfp/+}$ OT-II CD4^{+} T cells were cotransferred into congenic recipients, which subsequently received s.c. immunization with hen egg lysozyme (HEL)-ovalbumin (OVA)-conjugated protein. In the draining lymph nodes (LNs), YFP-Bcl6 upregulation began to be detected in some Hy10 B cells on day 3 of immunization (mice were immunized on day 0), and on day 4, Hy10 B cells were separated into two distinct populations of YFP^{hi} cells and YFP^{lo} cells (Figure 2A). The percentage of YFP^{hi} cells in Hy10 B cells reached a plateau on day 5, although absolute numbers of Hy10 B cells decreased between days 5 and 10. Majority of YFP^{hi} Hy10 B cells fell into the Fas^{hi}CD38^{lo} population by day 5. Upregulation of Fas and GL7 preceded Bcl6 upregulation, which was closely followed by CD38 downregulation (Figures 2A and 2C). In OT-II T cells YFP-Bcl6 expression was substantially upregulated by day 2, reached a maximum at approximately day 3, and then decreased toward day 10 (Figures 2B and 2D). After day 3, a majority of the YFP^{+} OT-II T cells were CXCR5^{hi}PD-1^{hi}. The percentage of CXCR5^{hi}PD-1^{hi} cells in OT-II T cells reached a maximum between days 3 and 4. Interestingly, not only YFP-Bcl6 expression in total OT-II T cells but also that in the CXCR5^{hi}PD-1^{hi} cell population decreased after day 3 (Figures 2B and 2D). Three weeks after immunization, most if not all of CXCR5^{hi}PD-1^{hi} OT-II T cells became YFP low or negative (Figure S2A). Consistent with the PP cell analysis in Figure 1C,

YFP-Bcl6 signals were well correlated with intracellular Bcl6 staining signals in *Bcl6*$^{yfp/+}$ Hy10 B cells and *Bcl6*$^{yfp/+}$ OT-II T cells (Figure S2B). Because Bcl6 is known to promote Tfh cell formation in a gene dose-dependent manner (Yu et al., 2009), we examined whether *Bcl6*$^{yfp/+}$ Tfh cells show abnormalities in formation kinetics or gene expression. As shown in Figure S2C, *Bcl6*$^{+/+}$ OT-II T cells and *Bcl6*$^{yfp/+}$ OT-II T cells formed similar numbers of Tfh cells at time points tested. In addition, Tfh cell-related gene expression was indistinguishable between *Bcl6*$^{+/+}$ OT-II Tfh cells and *Bcl6*$^{yfp/+}$ OT-II Tfh cells (Figures S2D and S2E). Intracellular Bcl6 staining of *Bcl6*$^{+/+}$ Hy10 B cells and *Bcl6*$^{+/+}$ OT-II T cells confirmed induction kinetics of Bcl6 revealed by use of *Bcl6*$^{yfp/+}$ cells (Figure S2F). Importantly, reduction of intracellular Bcl6 signals in *Bcl6*$^{+/+}$ OT-II Tfh cells was also observed between days 3 and 10 (Figure S2G). These results indicate that upregulation of Bcl6 protein in Ag-engaged CD4$^+$ T cells precedes that in Ag-engaged B cells. They also strongly suggest that after development of Tfh cells, which has been shown to require Bcl6, Bcl6 protein is gradually downmodulated in Tfh cells, whereas Bcl6 protein expression in GC B cells continues to be more uniformly high after development.

Ag-Engaged B Cells Upregulate Bcl6 Prior to Clustering in GCs

To understand where in the tissue Ag-engaged B cells and CD4$^+$ T cells upregulate Bcl6, we performed immunofluorescence staining of LN sections. Because YFP-Bcl6 fluorescence was not strong enough for histological analysis, we used polyclonal anti-green fluorescent protein (GFP) to detect YFP-Bcl6 expression in adoptively transferred avian lysozyme-specific MD4 BCR-transgenic B cells and OT-II T cells. We used MD4 B cells rather than Hy10 B cells for the technical simplicity of multistaining of LN sections with anti-IgM^a and anti-CD45.2. Unlike Hy10 B cells, MD4 B cells are not able to undergo class-switch recombination or somatic hypermutation in their transgenic BCR gene. Nonetheless, the previous studies suggest that MD4 B cells perform as a good model system for analysis of cell localization during the early phase of responses including clustering in GCs (Okada et al., 2005). Although the staining with anti-GFP produced background signals on some tissue structures, nuclear YFP-Bcl6 signals were convincingly detected in transferred *Bcl6*$^{yfp/+}$ cells, but not in *Bcl6*$^{+/+}$ cells, most prominently in the GC clusters (Figure 3A). When we analyzed LN sections of the day 3 time point, we noticed that MD4 B cells had not formed GC clusters in many follicles and were located mostly in the outer follicle, including interfollicular regions as previously described (Pereira et al., 2010). We detected YFP-Bcl6 expression in some of MD4 B cells in the outer follicle (Figures 3B and 3C), although the percentage of YFP$^+$ cells in MD4 B cells was variable among individual follicles at this time point, ranging from less than 10% to over 60%. Thus, Ag-engaged B cells upregulate Bcl6 in the outer follicle before forming GC clusters.

B-T Cell Interaction Requirements in Bcl6 Upregulation in Ag-Engaged CD4$^+$ T Cells and B Cells

On day 3, substantial numbers of OT-II T cells were found in the follicular regions, particularly in the outer follicle and interfollicular regions. Many of these cells in the follicular regions expressed YFP-Bcl6 (Figures 3B and 3D). OT-II T cells in the T cell zone appeared to be largely YFP negative. Nonetheless, YFP-Bcl6 expression, although usually weaker than that in OT-II T cells in the follicle, was detected in a small fraction of these cells in the T cell zone (Figures 3B and 3E), suggesting that Bcl6 protein expression by CD4$^+$ T cells might start in the T cell zone before cognate interactions with B cells. To test this, we transferred *Bcl6*$^{yfp/+}$ OT-II T cells to B cell-deficient mice. Consistent with previous studies (Haynes et al., 2007; Johnston et al., 2009; Poholek et al., 2010), Tfh cell development was severely compromised in B cell-deficient mice (Figure S3A). On day 5, we detected YFP-Bcl6 expression in transferred cells in the B cell-deficient recipients, but the maximum degrees of YFP-Bcl6 expressed in these cells were significantly decreased compared to *Bcl6*$^{yfp/+}$ OT-II T cells transferred to wild-type recipients. By day 10, YFP$^+$ OT-II T cells in B cell-deficient recipients became almost undetectable (Figure S3B). These results support that Ag-engaged CD4$^+$ T cells begin Bcl6 protein expression in the T cell zone and further increase it through interactions with Ag-presenting B cells to become Tfh cells.

We also performed the converse experiment to assess the impact of T cell deficiency on Bcl6 upregulation in B cells. B1-8^{hi} BCR gene targeted transgenic B cells specific for 4-hydroxy-3-nitrophenyl acetyl (NP) (Shih et al., 2002) were transferred to wild-type or TCR-α-deficient mice immunized with NP-OVA. *Bcl6*$^{yfp/+}$ B1-8^{hi} B cells transferred to wild-type recipients contained significant numbers of YFP-Bcl6^{hi} cells on days 5 and 10, whereas YFP-Bcl6^{hi} cells were few (day 5) or undetectable (day 10) in TCRα-deficient mice. In contrast, when recipients were immunized with thymus-independent type 2 Ag, NP-Ficoll, YFP-Bcl6^{hi} cells were induced both in wild-type mice and TCRα-deficient mice on day 5, but disappeared by day 10 (Figure S3C). These results are consistent with the previous studies on GC B cell formation (Vinuesa et al., 2010) and support the idea that T cell help is important for initial Bcl6 upregulation in B cells when Ag valency is relatively low and that sustainment of Bcl6^{hi} GC B cells absolutely requires T cell help regardless of Ag valency.

Hypomorphism of *Bcl6*$^{yfp/yfp}$ B Cells and *Bcl6*$^{yfp/yfp}$ CD4$^+$ T Cells

To establish an experimental system to examine the role of Bcl6 upregulation in pre-GC B cell dynamics, we analyzed *Bcl6*$^{yfp/yfp}$ MD4 B cells. As expected from the results described above (Figure S1D), *Bcl6*$^{yfp/yfp}$ MD4 B cells, which had been cotransferred with *Bcl6*$^{+/+}$ OT-II T cells into wild-type recipients immunized with HEL-OVA, were severely impaired in the formation of the Fas^{hi}CD38^{lo} GC B cell population compared to *Bcl6*$^{yfp/+}$ MD4 B cells (Figure 4A). Interestingly, the YFP^{hi} population of *Bcl6*$^{yfp/yfp}$ MD4 B cells was nearly abolished (Figure 4A), suggesting that YFP-Bcl6 is impaired in promoting survival of B cells committed into the GC pathway. Indeed, the percentage of annexin V$^+$ cells in YFP^{hi} *Bcl6*$^{yfp/yfp}$ B cells (12 ± 0.82%, n = 3), although we could analyze only small numbers of these cells, was significantly higher than in YFP^{hi} *Bcl6*$^{yfp/+}$ B cells (6.25% ± 1.47%, n = 3, p = 0.022). After 4 days of immunization, *Bcl6*$^{yfp/yfp}$ MD4 B cells expressing GFP were observed to be unable to accumulate in GCs, whereas GFP$^+$ *Bcl6*$^{+/+}$ MD4 B cells efficiently did so (Figure 4B). These results confirm that *Bcl6*$^{yfp/yfp}$

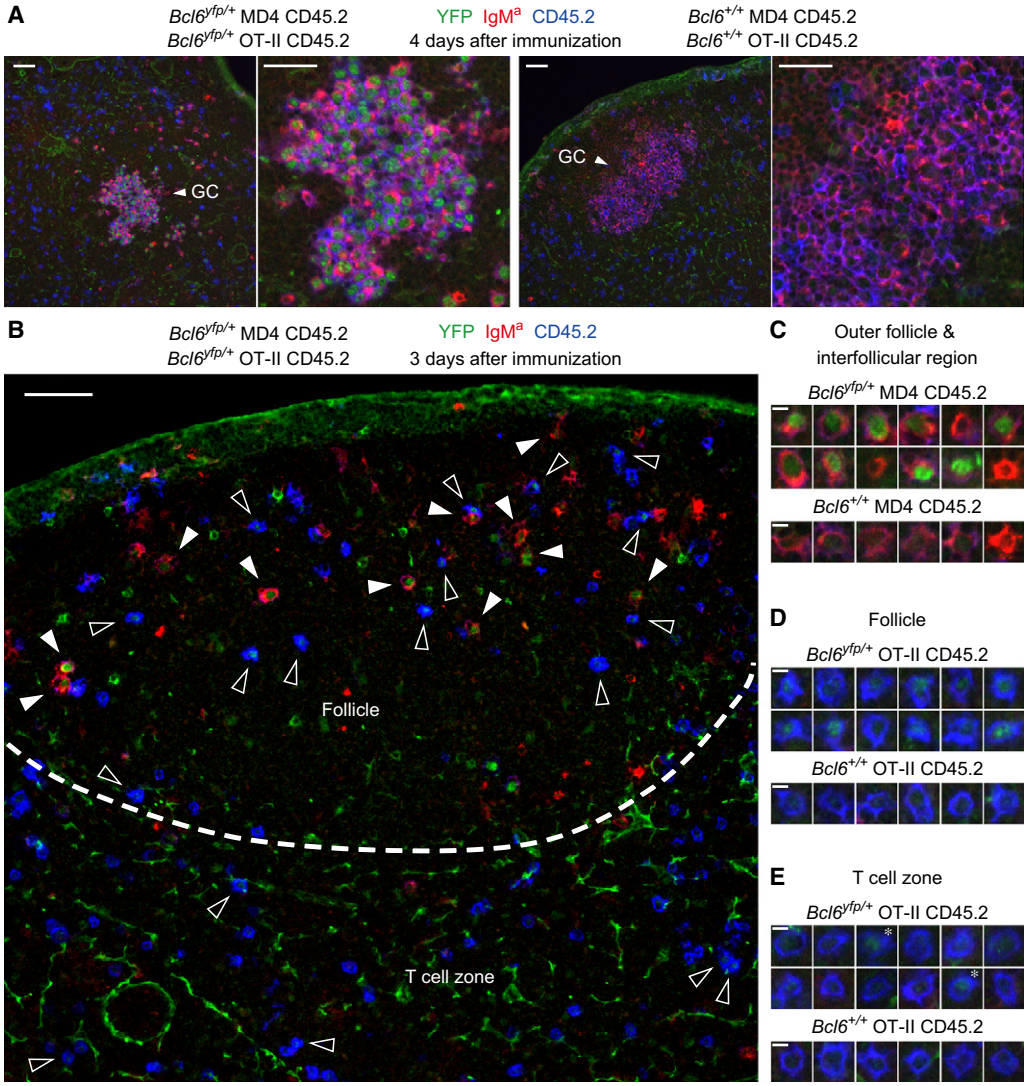

Figure 3. Detection of YFP-Bcl6 in Pre-GC B Cells and Helper T Cells

Bcl6$^{yfp/+}$ or *Bcl6*$^{+/+}$ MD4 B cells and *Bcl6*$^{yfp/+}$ or *Bcl6*$^{+/+}$ OT-II T cells were transferred to CD45.1 congenic mice, and immunized with HEL-OVA in CFA. LN sections were stained with anti-GFP to detect YFP-Bcl6, for IgM^{a} to identify MD4 B cells, and for CD45.2 to identify OT-II T cells and MD4 B cells. The scale bar represents 50 μm (A and B) and 5 μm (C–E).

(A) GCs formed on day 4 are shown at two different magnifications.

(B) YFP-Bcl6-expressing MD4 B cells and OT-II T cells on day 3 are marked by filled and open arrowheads, respectively. The dotted line shows approximate location of the boundary between the B cell follicle and the T cell zone.

(C–E) Representative images of MD4 B cells and OT-II T cells on day 3. In (E), cells with weak but detectable YFP signals are marked with asterisks.

MD4 B cells are useful for functional analysis of Bcl6 upregulation in terms of B cell dynamics.

We also found that *Bcl6*$^{yfp/yfp}$ OT-II T cells were defective in the formation of the cells with the highest expression of CXCR5 and PD-1 (Figure 4A). Two-photon microscopy of LNs and subsequent flow cytometric analysis of the same LNs showed that *Bcl6*$^{yfp/yfp}$ OT-II T cells expressing cyan fluorescent protein (CFP) were reduced in the follicular mantle zone and more severely in the GCs compared to GFP^{+} *Bcl6*$^{+/+}$ or CFP^{+} *Bcl6*$^{+/+}$ OT-II T cells (Figures 4C and 4D, and Movie S1). These results support that Tfh cells with the highest expression of CXCR5 and PD-1 are the Tfh cell population inhabiting GCs. In addition, we examined the capacity of *Bcl6*$^{yfp/yfp}$ OT-II T cells to support GC B cell development by cotransfer of purified *Bcl6*$^{yfp/+}$ Hy10 B cells with *Bcl6*$^{+/+}$ or *Bcl6*$^{yfp/yfp}$ OT-II T cells into *Bcl6*$^{+/+}$ or *Bcl6*$^{yfp/yfp}$ recipients. The number of YFP^{hi} Hy10 GC B cells was decreased when cognate helper T cells were of the *Bcl6*$^{yfp/yfp}$ genotype (Figure S4A). Conversely, we also analyzed *Bcl6*$^{yfp/+}$ OT-II T cells that had been purified and transferred into wild-type or *Bcl6*$^{yfp/yfp}$ recipients. Endogenous B cells in *Bcl6*$^{yfp/yfp}$ recipient mice failed to develop GC B cells as expected. However, this near complete absence of GC B cells did not significantly affect YFP-Bcl6 upregulation in or the Tfh cell formation from transferred *Bcl6*$^{yfp/+}$ OT-II T cells

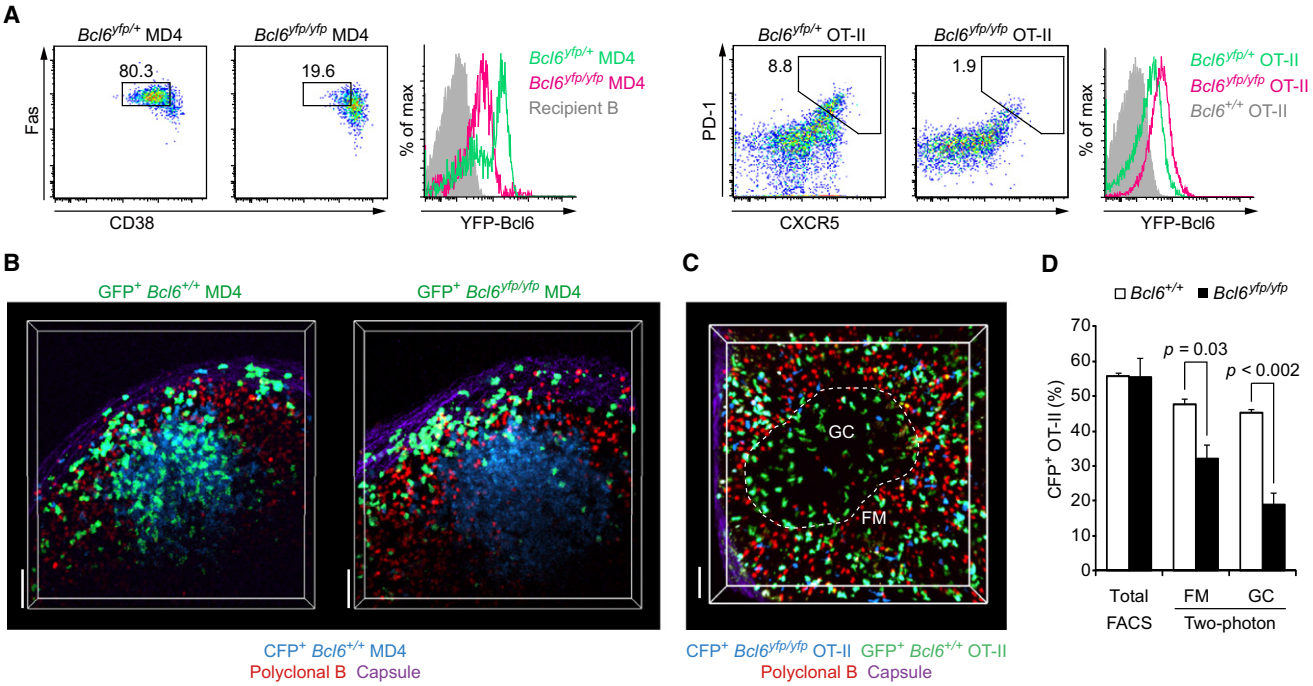

Figure 4. *Bcl6*$^{yfp/yfp}$ B and T Cells Show Hypomorphic Phenotypes

(A) Flow cytometric analysis of transferred *Bcl6*$^{yfp/+}$ or *Bcl6*$^{yfp/yfp}$ MD4 B cells and *Bcl6*$^{yfp/+}$ or *Bcl6*$^{yfp/yfp}$ OT-II T cells in the draining LNs on day 7.

(B) Two-photon images of GCs in intact LNs. CFP$^+$ *Bcl6*$^{+/+}$ MD4 cells, GFP$^+$ *Bcl6*$^{+/+}$, or GFP$^+$ *Bcl6*$^{yfp/yfp}$ B cells, and rhodamine-labeled polyclonal B cells were transferred and visualized 4.5 days after immunization with HEL-OVA in alum. The images are 45 μm z projections. The scale bar represents 50 μm.

(C) Two-photon imaging of a GC in an intact LN on day 7 after immunization with NP-OVA in alum (see also Movie S1). CFP$^+$ *Bcl6*$^{yfp/yfp}$ (C) or CFP$^+$ *Bcl6*$^{+/+}$ (not shown) OT-II T cells, GFP$^+$ *Bcl6*$^{+/+}$ OT-II T cells, and rhodamine-labeled polyclonal B cells were cotransferred and visualized in recipient LNs. The image is a 105 μm z projection. FM: follicular mantle. The scale bar represents 50 μm.

(D) Relative frequencies of *Bcl6*$^{+/+}$ OT-II T cells and *Bcl6*$^{yfp/yfp}$ OT-II T cells in the FM and GC. CFP$^+$ *Bcl6*$^{yfp/yfp}$ or CFP$^+$ *Bcl6*$^{+/+}$ OT-II T cells and GFP$^+$ *Bcl6*$^{+/+}$ OT-II T cells located in the FM and GC regions were counted in two-photon images of LNs including (C), and the percentage of CFP$^+$ cells within total OT-II T cells was calculated. Cells from the same LNs were subsequently analyzed by flow cytometry, and the percentage of CFP$^+$ cells in the total OT-II T cells in the LNs was calculated. Data represent mean ± SEM.

The data are representative (A–C) or accumulation (D) of more than three experiments.

(Figures S4B and S4C). These results suggest that the generation or maintenance of Tfh cells, at least in the early phase of the Ab response, does not depend on their interactions with GC B cells, whereas GC B cell development is sensitive to the number of Tfh cells with the highest CXCR5 and PD-1 expression.

Bcl6 Upregulation Is Essential for Entry of Pre-GC B Cells to GC Clusters

Having established that *Bcl6*$^{yfp/yfp}$ MD4 B cells are severely impaired in the formation of YFP^{hi} GC B cells, we examined whether the failure of these cells to be localized in GCs was due to the blocked entry into the GC clusters. To test this possibility, we used a protocol modified from the previous study that reported entry of newly activated B cells into preformed GCs (Schwickert et al., 2009). Two-photon imaging was performed for the LNs in which CFP$^+$ *Bcl6*$^{+/+}$ MD4 B cells had already formed GC clusters, whereas the majority of GFP$^+$ *Bcl6*$^{+/+}$ or GFP$^+$ *Bcl6*$^{yfp/yfp}$ MD4 B cells were still in the outer follicle regions. During the 1 hr imaging period, a fraction of GFP$^+$ *Bcl6*$^{+/+}$ MD4 B cells were observed to enter the GC area demarcated by CFP (Figures 5A– 5C; Movie S2 and Movie S3). Egress of these cells from the GC area was less efficient than entry to the GC (Figure 5C), confirming that these cells were in the course of clustering into the GC. Remarkably, entry of GFP$^+$ *Bcl6*$^{yfp/yfp}$ MD4 B cells to the GC area was severely impaired, although these cells could access to the border of GCs (Figures 5A–5C; Movie S2 and Movie S3). The number of GFP$^+$ *Bcl6*$^{yfp/yfp}$ MD4 B cells in the GC area was too small to determine the egress efficiency from the GC. CXCR5 expression was not significantly different between *Bcl6*$^{yfp/+}$ B cells, *Bcl6*$^{yfp/yfp}$ B cells, and *Bcl6*$^{+/+}$ B cells (Figure S5A and data not shown). GC B cells are known to upregulate CXCR4 (Allen et al., 2004), and this upregulation was impaired in YFP^{hi} *Bcl6*$^{yfp/yfp}$ B cells (Figure S5A). Importantly, *Gpr183* expression on day 3.5 was already downregulated in *Bcl6*$^{yfp/+}$ MD4 B cells after YFP-Bcl6 upregulation but not in *Bcl6*$^{yfp/yfp}$ MD4 B cells (Figures S5B and S5C). These observations strongly suggest that Bcl6 upregulation in B cells in the outer follicle enables these cells to migrate into GC clusters.

A Role for Bcl6 in B Cells in Sustaining Conjugation with Helper T Cells

We also examined whether Bcl6 upregulation has impacts on dynamics of B cell-T cell interactions by tracking contacts between *Bcl6*$^{+/+}$ or *Bcl6*$^{yfp/yfp}$ MD4 B cells and OT-II T cells in

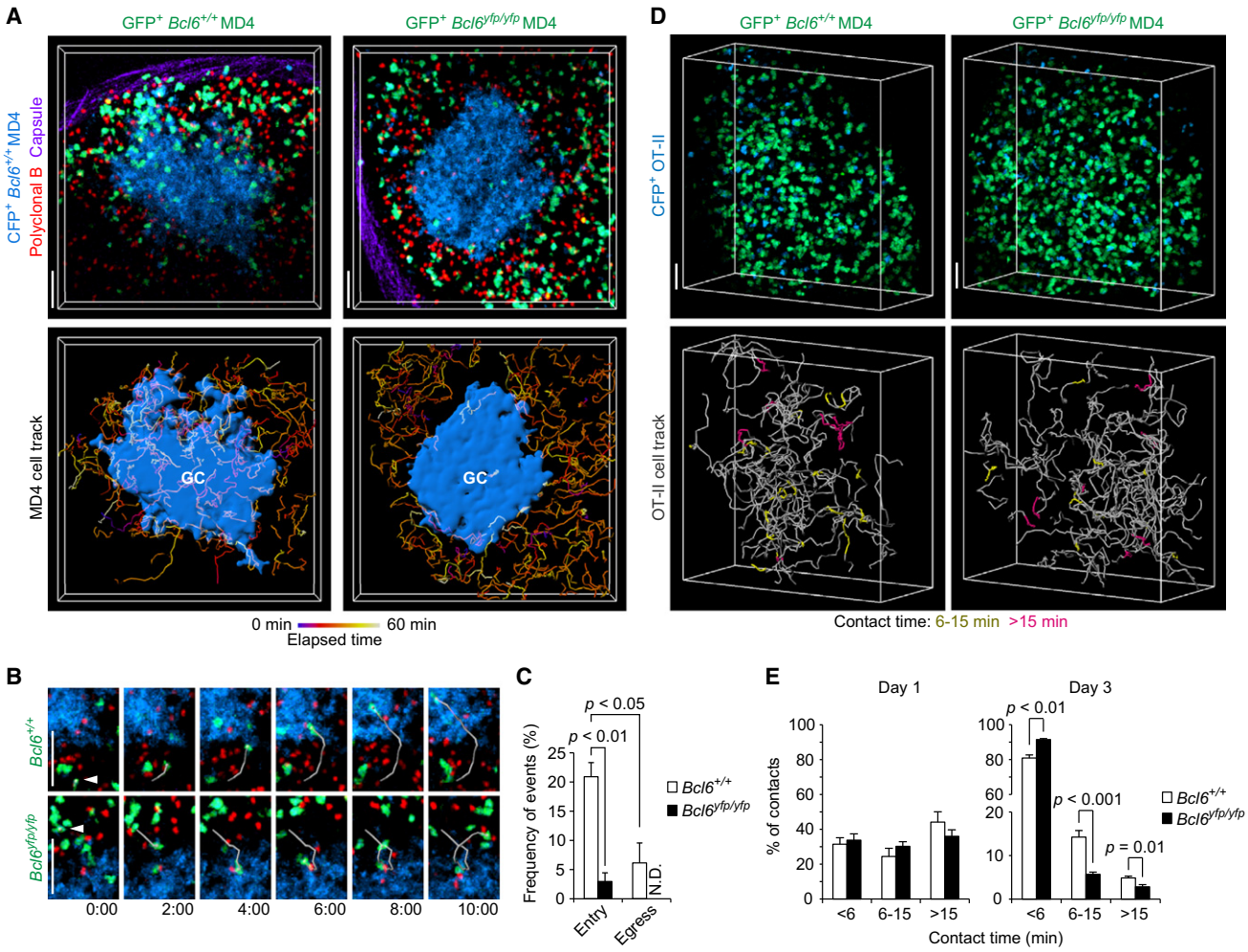

Figure 5. *Bcl6*$^{yfp/yfp}$ B Cells Are Defective in Entry to GCs and Stable B Cell-T Cell Interaction

(A) Two-photon imaging of the B cell entry into the pre-formed GC. Mice co-transferred with CFP$^+$ MD4 B cells and OT-II T cells were immunized with HEL-OVA in alum. After 36 hr, GFP$^+$ *Bcl6*$^{+/+}$ or GFP$^+$ *Bcl6*$^{yfp/yfp}$ MD4 B cells were cotransferred with rhodamine-loaded polyclonal B cells into the immunized mice. The draining LNs were subjected to imaging 3.5 days after the second transfer (see also Movie S2). The top panels are representative images from 60 min recordings. The bottom panels show the surface of GCs reconstructed from the CFP images and the trajectories of GFP$^+$ MD4 B cells. The images are 30 μm z projections. The scale bar represents 50 μm.

(B) Time-lapse images of a GFP$^+$ *Bcl6*$^{+/+}$ MD4 B cell and a *Bcl6*$^{yfp/yfp}$ MD4 B cell accessing the GC border. Arrowheads in the far left panels indicate the tracked MD4 B cells (see also Movie S3). Images are presented as 18 μm z projections; elapsed time is presented as mm:ss. The scale bar represents 50 μm.

(C) Relative frequency of the GFP$^+$ *Bcl6*$^{+/+}$ MD4 B cell and *Bcl6*$^{yfp/yfp}$ MD4 B cell entry to and egress from GCs. The percentages of entering (or egressing) cells in cells that accessed the GC border from the outside (or inside) of GCs and left the border in either way are shown as the entry (or egress) frequency (mean ± SEM, n = 3 LNs, 69 and 58 total events scored in *Bcl6*$^{+/+}$ and *Bcl6*$^{yfp/yfp}$ B cell entry analysis, respectively, and 44 total events scored in *Bcl6*$^{+/+}$ B cell egress analysis). N.D., not determined.

(D) Two-photon imaging of the B cell-T cell interaction. GFP$^+$ *Bcl6*$^{+/+}$ MD4 B cells or GFP$^+$ *Bcl6*$^{yfp/yfp}$ MD4 B cells were cotransferred with CFP$^+$ OT-II T cells, and recipients were immunized with HEL-OVA in alum. On day 3, the draining LNs were subjected to imaging. Fluorescence images and representative OT-II T cell tracks were shown. While on the yellow and pink tracks, OT-II T cells were observed to interact with MD4 B cells for 6–15 min and for more than 15 min, respectively (see also Movie S4). The scale bar represents 50 μm.

(E) Duration of contacts between *Bcl6*$^{+/+}$ or *Bcl6*$^{yfp/yfp}$ MD4 B cells and OT-II T cells at the indicated time points (mean ± SEM, n = 4 for day 1 and n = 5 for day 3; 119 and 78 contacts for day 1, and 866 and 845 contacts for day 3 scored for *Bcl6*$^{+/+}$ and *Bcl6*$^{yfp/yfp}$ B cells, respectively).

the LNs (Figure 5D and Movie S4). We categorized the contacts into three groups in terms of the contact time: shorter than 6 min, 6 to 15 min, and longer than 15 min, on the basis of the previous findings that noncognate B cell-T cell contacts hardly last more than 6 min and that cognate interactions can be sustained for more than 15 min in a signaling lymphocytic activation molecule (SLAM) family protein-dependent manner (Cannons et al., 2010; Okada et al., 2005; Qi et al., 2008). One day after immunization, the contact time for *Bcl6*$^{yfp/yfp}$ MD4 B cells was not significantly different from that for *Bcl6*$^{+/+}$ MD4 B cells (Figure 5E, Figures S5D and S5E, and Movie S5). However, 3 days after immunization, when majority of both *Bcl6*$^{+/+}$ MD4 B cells and *Bcl6*$^{yfp/yfp}$

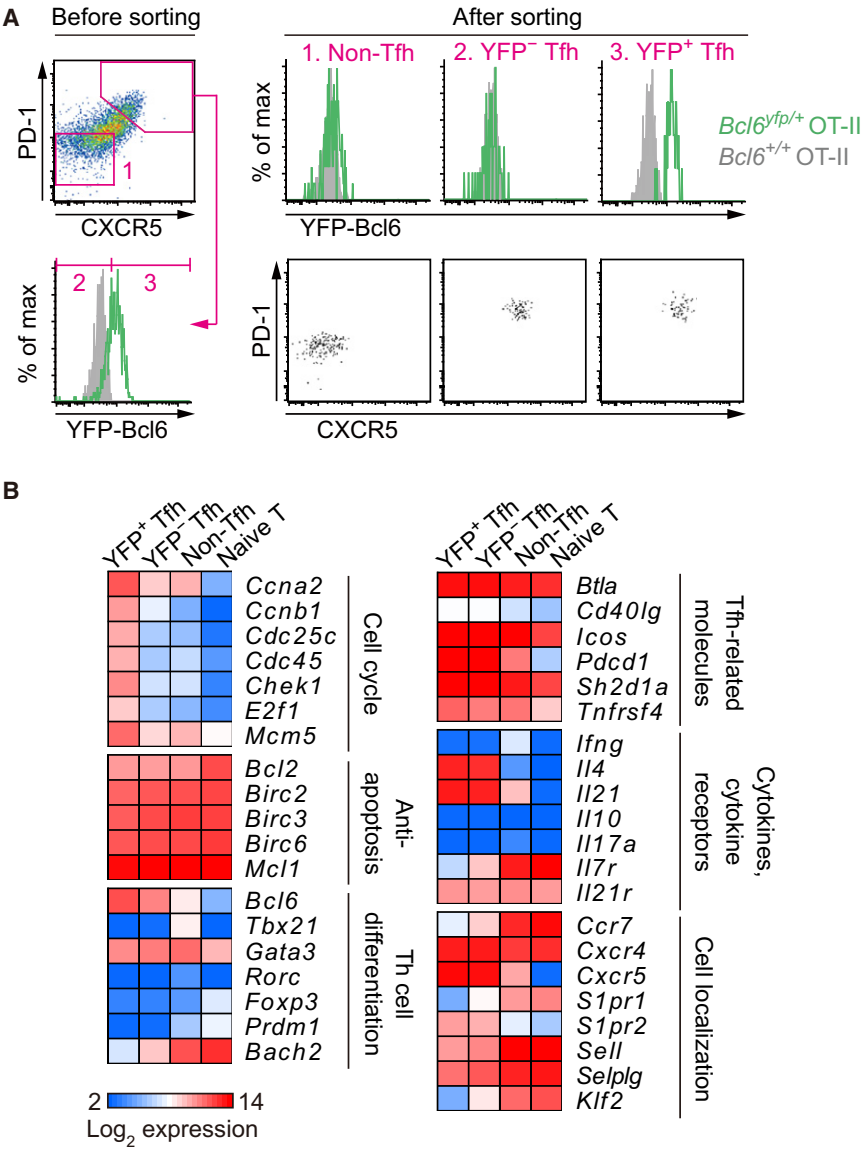

Figure 6. Gene Expression Analysis of Bcl6-Low Tfh Cells

Transferred *Bcl6*$^{yfp/+}$ OT-II T cells were sorted from draining LN cells 7 or 10 days after immunization with NP-OVA in CFA. YFP$^+$ Tfh cells, YFP$^-$ Tfh cells, and non-Tfh cells were examined for mRNA expression by microarray analysis.

(A) Flow cytometry of OT-II T cells before and after sorting.

(B) Heat-map of mRNA expression. Mean values of microarray data for the Tfh cell types (n = 4), non-Tfh cells (n = 3), and naive CD4$^+$ T cells (n = 2) are shown (see also Table S1).

MD4 B cells were located in the outer follicle, the frequency of contacts lasting more than 6 min was significantly lower for *Bcl6*$^{yfp/yfp}$ MD4 B cells than *Bcl6*$^{+/+}$ MD4 B cells (Figures 5D and 5E, Figure S5E, and Movie S4). These data together with the observation that Ag-engaged B cells began to upregulate Bcl6 3 days after immunization (Figure 2 and Figure 3) suggest that Bcl6 upregulation in Ag-engaged B cells contributes to sustaining conjugation with helper T cells.

Bcl6-Low Tfh Cells Are Detectable in the GC and Accelerated to Become Proliferatively Quiescent and Express IL-7 Receptor

As our results suggesting that Tfh cells downmodulate Bcl6 after their development were unexpected, we sought to understand functional characteristics of these Bcl6-low Tfh cells. To this end, we sorted YFP$^+$ Tfh cells, YFP$^-$ Tfh cells, and non-Tfh cells derived from *Bcl6*$^{yfp/+}$ OT-II T cells (Figure 6A). The gene expression profiles of these cells were investigated by microarray analysis (Figure 6B and Table S1). The overall gene expression pattern of YFP$^-$ Tfh cells was much closer to that of YFP$^+$ Tfh cells than that of non-Tfh cells (Figure S6). The most striking difference between YFP$^+$ Tfh cells and YFP$^-$ Tfh cells was that expression of genes whose upregulation is associated with cell cycle progression was decreased in YFP$^-$ Tfh cells (Figure 6B and Table S1). Indeed, DNA content analysis revealed that proliferation of YFP$^-$ Tfh cells was more rapidly decreased than that of YFP$^+$ Tfh cells between days 4 and 7 (Figure 7A). Surprisingly, mRNA expression of the transcription factors important for helper T cell differentiation was not much changed between the two Tfh cell types: *Bcl6* mRNA remained abundant in YFP$^-$ Tfh cells although slightly reduced compared to YFP$^+$ Tfh cells; expression of *Tbx21* (T-bet), *Rorc* (RORγt), and *Prdm1* (Blimp-1) that Bcl6 can repress was similarly low in the both Tfh cell types. Expression of *Bach2* encoding another repressor of *Prdm1* expression in B cells (Martins and Calame, 2008) was higher in YFP$^-$ Tfh cells than in YFP$^+$ Tfh cells. The other Tfh-related genes, including *Cxcr5*, *Pdcd1* (PD-1), *Il4*, and *Il21*, were highly expressed in the both Tfh cell types compared to non-Tfh cells or naive cells. Interestingly, transcripts of *Il7r*, *Ccr7*, *S1pr1* (sphingoshin-1-phosphate receptor-1), and *Klf2* (Kruppel-like factor 2, a transcription factor critical for *S1pr1* expression) (Carlson et al., 2006) were modestly but noticeably upregulated in YFP$^-$ Tfh cells compared to YFP$^+$ Tfh cells (Figure 6B and Table S1).

Relatively higher surface expression of the IL-7 receptor alpha chain (CD127) in YFP$^-$ Tfh cells compared to YFP$^+$ Tfh cells was observed for OT-II Tfh cells (Figure 7B), and also for endogenous Tfh cells in spleen (Figure S7A) and PPs (data not shown). Three weeks after immunization, the majority of *Bcl6*$^{yfp/+}$ OT-II Tfh cells (58% ± 4.0%, n = 3) or *Bcl6*$^{+/+}$ OT-II Tfh cells (56% ± 7.6%, n = 3) were CD127 positive. Intracellular Bcl6 staining of both *Bcl6*$^{+/+}$

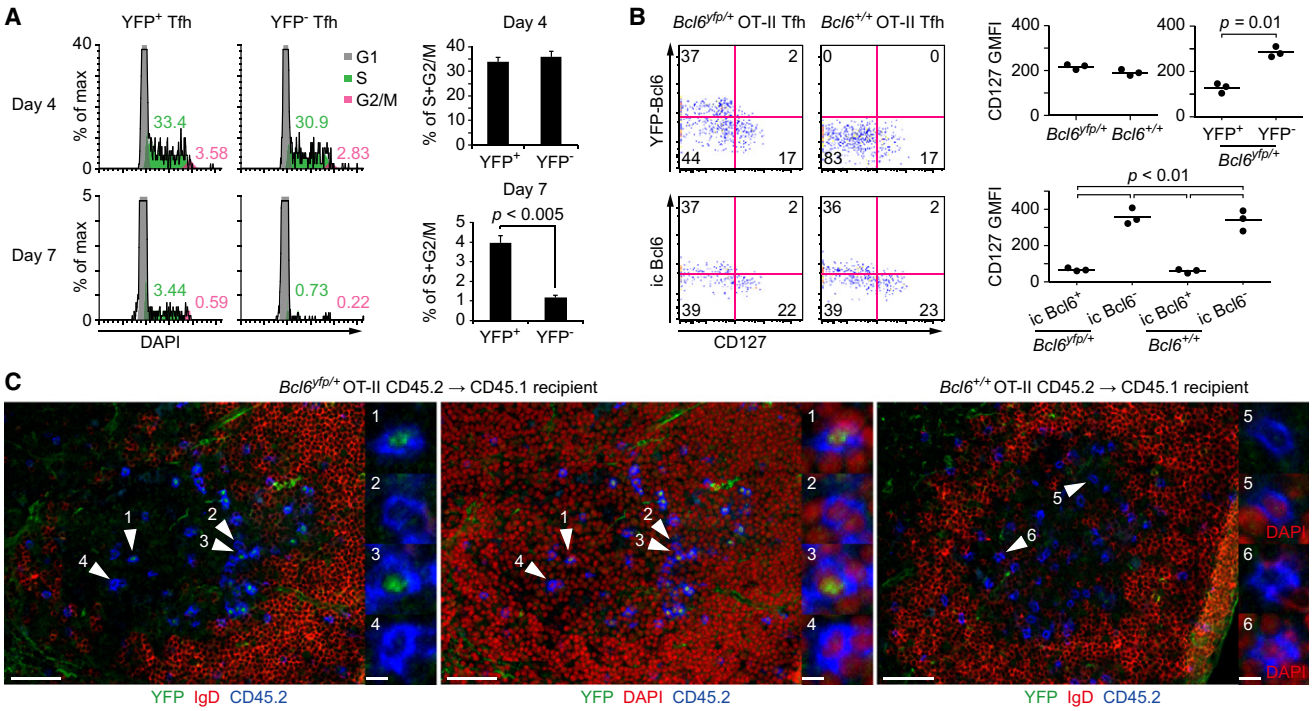

Figure 7. Bcl6-Low Tfh Cells Are Detectable in the GC and Accelerated to Become Proliferatively Quiescent, and Express IL-7 Receptor

(A) Cell cycle analysis of YFP$^+$ Tfh and YFP$^-$ Tfh cells. Mice transferred with *Bcl6*$^{yfp/+}$ OT-II cells were immunized with NP-OVA in CFA. On day 4 or day 7, draining LN cells were stained with 4'6-diamidino-2-phenylindole (DAPI) and the Abs against the Tfh surface markers. Representative histograms and the percentage of cells in the S and G2/M phases within YFP$^+$ or YFP$^-$ Tfh cells are shown (mean ± SEM, n = 4).

(B) Flow cytometric analysis of CD127 and Bcl6 expression in *Bcl6*$^{yfp/+}$ OT-II Tfh cells and *Bcl6*$^{+/+}$ OT-II Tfh cells on day 9 of i.p. immunization with NP-OVA in alum.

(C) *Bcl6*$^{yfp/+}$ or *Bcl6*$^{+/+}$ OT-II T cells were transferred to CD45.1 recipients that were immunized with OVA in alum and sacrificed 10 days after immunization. Draining LN sections were stained with anti-GFP to detect YFP-Bcl6, for IgD to demarcate GCs, for CD45.2 to identify OT-II T cells, and with DAPI for cell nuclei. Scale bars represent 50 μm (left panels) and 5 μm (right panels).

Tfh cells and *Bcl6*$^{yfp/+}$ Tfh cells confirmed the preferential expression of CD127 in Bcl6-low Tfh cells (Figure 7B). Surface expression of CCR7 was similarly low between YFP$^+$ Tfh cells and YFP$^-$ Tfh cells despite the difference in transcript expression (Figure S7B). We also cultured these sorted Tfh cell types in the presence of phorbol ester and ionomycin and found that the both Tfh cell types were similarly capable of secreting IL-4 (data not shown). Lastly, we examined whether YFP$^+$ and YFP$^-$ Tfh cells were both present in the GC. Immunofluorescence staining of *Bcl6*$^{yfp/+}$ OT-II T cells in the recipient LNs showed that there were both YFP$^+$ and YFP$^-$ OT-II T cells in the GC (Figure 7C). Various magnitudes of Bcl6 expression were also observed for *Bcl6*$^{+/+}$ OT-II T cells in GCs by staining with anti-Bcl6 (Figure S7C). Taken together, these results suggest that after downmodulation of Bcl6 protein Tfh cells still reside in the GC and remain capable of supporting the B cell response and that these cells rapidly decrease proliferation and gradually enhance their IL-7 responsiveness and migration potential including that for egress from the LN to circulation.

DISCUSSION

The regulation of Bcl6 expression in B cells, T cells, and other immune cells is crucial for successful immune responses, and its dysregulation can lead to inflammatory diseases and lymphoma development (Klein and Dalla-Favera, 2008; Shaffer et al., 2001). Bcl6 expression is known to be controlled by the various posttranscriptional mechanisms (Basso and Dalla-Favera, 2010; Crotty et al., 2010). Thus, it has been recognized that detection of Bcl6 protein rather than *Bcl6* mRNA is important for understanding the Bcl6-dependent cellular functions. The present study describes the tracking of Bcl6 protein expression in individual Ag-engaged B cells and helper T cells during Ab responses, which was facilitated by the Bcl6 reporter mouse whose *Bcl6* gene locus encodes YFP-Bcl6 fusion protein.

A concern with this reporter animal was that the fusion protein might display altered stability compared to that of wild-type Bcl6 protein. However, *Bcl6*$^{yfp/+}$ GC B cells or *Bcl6*$^{yfp/+}$ Tfh cells expressed YFP-Bcl6 in similar amounts to wild-type Bcl6, suggesting that YFP-Bcl6 serves as the reporter for wild-type Bcl6 expression in cells from heterozygous animals. Intracellular Bcl6 staining of *Bcl6*$^{yfp/+}$ GC B cells and Tfh cells further confirmed this view. However, analysis of cells from homozygous animals indicated that YFP-Bcl6 was functionally compromised, possibly because fusion with YFP near the BTB domain of Bcl6 might impair recruitment of the corepressor molecules or disrupt the formation of Bcl6 homodimers or heterodimers with other BTB domain-containing transcription factors (Basso and Dalla-Favera, 2010).

Multidirectional differentiation of Ag-engaged B cells sets up the rapid Ab production by extrafollicular plasma cells and the

sustained, high-affinity Ab response by GC B cells. It is currently unknown how B cell commitment to GC B cell differentiation versus extrafollicular plasmablast differentiation is determined. The recent discovery by two groups that EBI-2 is important for localization of Ag-engaged B cells in the outer follicle and for the development of extrafollicular plasma cells suggests that the outer follicle is the important site for commitment into the plasma cell pathway (Gatto et al., 2009; Pereira et al., 2009). The same groups have also reported that downregulation of EBI-2 in GC B cells, which is most likely achieved by the Bcl6-dependent repression, plays a role in their clustering within the inner follicle (Gatto et al., 2009; Pereira et al., 2009). There was an uncertainty, however, regarding where the commitment to GC B cell differentiation takes place because it was still possible that some Ag-engaged B cells might briefly access the inner follicle to upregulate Bcl6 for the retention in the region. Our finding that Bcl6 is upregulated in Ag-engaged B cells in the outer follicle prior to GC clustering strongly suggests that the GC commitment occurs in the outer follicle region. Moreover, B cells defective in developing a Bcl6-high population showed impaired entry into the GC cluster, suggesting that EBI-2 downregulation and other Bcl6-dependent changes in responsiveness to spatial cues begin in pre-GC B cells while they are still in the outer follicle. In fact, downregulation of *Gpr183* expression was observed for $Bcl6^{yfp/+}$ MD4 B cells, but not for $Bcl6^{yfp/yfp}$ MD4 B cells, at this early time point when majority of them are still in the outer follicle. CXCR4 upregulation was also impaired in $Bcl6^{yfp/yfp}$ MD4 B cells. It has been reported that CXCR4-deficient GC B cells are able to form clusters in the inner follicle, although they are defective in the dark-zone/light-zone separation within GCs (Allen et al., 2004). Therefore, this effect is probably not the primary cause of the impairment in initial GC entry of $Bcl6^{yfp/yfp}$ B cells. Nonetheless, it is not excluded that CXCR4 upregulation may play a minor but overlapping role with EBI-2 downregulation. Bcl6 upregulation is most likely important for retention in the GC as well, although our analysis did not allow us to conclude on this point. It is also worth mentioning that the inability of $Bcl6^{yfp/yfp}$ B cells to accumulate in GC clusters may lead to their failure to receive survival signals and may contribute to the augmented rate of their death.

At the time when B cells start upregulating Bcl6 in the outer follicle, the frequency of sustained cognate B-T cell interactions is decreased compared to earlier time points. Later in the mature GC, the frequency of sustained cognate interactions between GC B cells and GC Tfh cells is further decreased (Allen et al., 2007b). Unexpectedly, our results suggest that Bcl6 upregulation in Ag-engaged B cells has a positive effect for sustaining their conjugation with helper T cells. The SLAM family proteins, CD84 and Ly106, might be the attractive candidate molecules responsible for this effect of Bcl6 upregulation since these molecules have been reported to be important for the stable B-T conjugations, especially for those lasting more than 15 min (Cannons et al., 2010). However, the decreased frequency was similarly observed between conjugations tracked for 6–15 min and those longer than 15 min when B cells were defective in upregulation and function of Bcl6. Therefore, it seems more likely that Bcl6 upregulation enhance integrin-dependent conjugation of B cells and helper T cells (Cannons et al., 2010). Bcl6 expression can also regulate costimulatory signals that may affect B-T interaction dynamics. Alternatively, Bcl6 expression may enhance Ag-presentation by B cells to facilitate cognate interactions with helper T cells. Future studies will be needed to clarify molecular mechanisms and physiological roles for Bcl6-dependent enhancement of B-T conjugations.

Bcl6 protein expression in $CD4^+$ T cells seems to be well correlated with *Bcl6* mRNA expression in the course of Tfh cell development. It has been reported that *Bcl6* mRNA can be partially upregulated in Ag-engaged $CD4^+$ T cells in the absence of B cells, although these $CD4^+$ T cells do not develop into Tfh cells (Poholek et al., 2010). Our results show that Bcl6 protein is also partially upregulated in Ag-engaged $CD4^+$ T cells in the absence of B cells. $CD4^+$ T cells further upregulate *Bcl6* expression to become Tfh cells usually through cognate interactions with B cells (Crotty et al., 2010; Deenick et al., 2010; Poholek et al., 2010), and this is also consistent with our analysis with the YFP-Bcl6 mouse. Unexpectedly, however, our results suggest that many Tfh cells start to decrease Bcl6 protein expression before or around the time of mature GC formation, and almost all the antigen-specific Tfh cells downmodulate Bcl6 at the later time point. The reduction of Bcl6 protein expression might not accompany a matched loss of transcript expression. Future studies need to address whether posttranscriptional mechanisms operate for regulating Bcl6 protein expression in these cells.

A marked phenotype of Bcl6-low Tfh cells was the accelerated termination of proliferation, while they seemed to remain capable of providing help to B cells in terms of cytokine expression and their appearance in the GC. The rapid termination of proliferation most likely contributes to limiting the number of Tfh cells for selection of GC B cells (Allen et al., 2007a; Victora et al., 2010) and preventing dysregulated GC expansion that may cause the autoimmune diseases (Vinuesa et al., 2009). Because Bcl6 function has been implicated in cellular proliferation, it is proposed that the enhanced quiescence of YFP^- Tfh cells is a result of the reduction of Bcl6 protein expression. However, our results may not fit the manner in which Bcl6 has been reported to promote cellular proliferation. A known target gene of Bcl6-dependent repression pertaining to GC B cell proliferation is *Cdkn1b* encoding a cell cycle inhibitor p27kip1 (Basso and Dalla-Favera, 2010). However, we did not see upregulation of *Cdkn1b* transcripts in YFP^- Tfh cells. Yet, we detected in these cells downregulation of many genes whose upregulation is associated with cell cycle progression. One of them was *Chek1* involved in the DNA-damage response. In proliferating GC B cells, on the contrary, Bcl6 is thought to repress *Chek1* to facilitate somatic mutations in the immunoglobulin genes (Basso and Dalla-Favera, 2010). Thus, cell cycle-related gene targets of Bcl6 in Tfh cells are not completely overlapped with those in GC B cells.

It was recently observed that a small fraction of Tfh cells in GCs expressed IFN-γ after *Leishmania major* infection (Reinhardt et al., 2009) and that lymphocytic choriomeningitis virus-specific Tfh cells expressed T-bet and IFN-γ (Johnston et al., 2009). In addition, it was reported that in the autoimmune conditions GC Tfh cells produced IL-17 (Bauquet et al., 2009; Hsu et al., 2008). Because Bcl6 was reported to inhibit T-bet and RORγt expression and/or function (Linterman and Vinuesa, 2010; Nurieva et al., 2009; Yu et al., 2009), it seemed possible that YFP^- Tfh cells might upregulate expression of the

transcription factors and/or cytokines of Th1 and Th17 cells. However, this was not the case at least in our immunization setting using the model Ags. Future studies will need to address whether YFP$^-$ Tfh cells are able to acquire Th1 and Th17 effector functions in response to pathogens or in autoimmune conditions. The transcription factor Blimp-1 has been suggested to be important for homeostasis of effector helper T cells other than Tfh cells (Crotty et al., 2010; Martins and Calame, 2008; Nutt et al., 2007). *Prdm1* expression, which can be repressed by Bcl6, was also kept low in Bcl6-low Tfh cells. This is consistent with the observation that *Bcl6* transcript was still abundant in these cells, given that Blimp-1 is known to inhibit *Bcl6* expression (Crotty et al., 2010; Martins and Calame, 2008). Repression of *Prdm-1* expression after the reduction of Bcl6 protein may involve other transcription factors including Bach2 (Martins and Calame, 2008).

Our results suggest that almost all of the Ag-specific Tfh cells become Bcl6 low after weeks of immunization. Because the Bcl6-low Tfh cells are cell cycle quiescent and express IL-7 receptor, we propose that these cells are precursors of memory helper T cells derived from Tfh cells. CXCR5$^+$ memory helper T cells that are resident in draining LNs have been observed in the late phase of the polyclonal helper T cell response (Fazilleau et al., 2007). These memory Tfh cells have decreased Tfh cytokine mRNA expression and differ from Bcl6-low Tfh cells in this sense. Because it is highly possible that Bcl6-low Tfh cells are still in the course of changing gene expression, these cells may become more resembled to the LN resident memory Tfh cells at later time points. Nonetheless, Bcl6-low Tfh cells may be also forming a distinct subset of memory helper T cells because they (or a fraction of them) upregulate *Klf2* and *S1pr1* expression, which may allow them to eventually exit from the LN (Carlson et al., 2006; Cyster, 2005) to become recirculating CXCR5$^+$ helper T cells (Förster et al., 1994; Morita et al., 2011; Simpson et al., 2010) or to reside in other tissues like the bone marrow (Tokoyoda et al., 2009).

EXPERIMENTAL PROCEDURES

Mice

Mice were housed under specific pathogen-free conditions and used according to the guidelines of the RIKEN Animal Research Committee. The *Bcl6^{yfp}* mouse generation and the other mice are described in the Supplemental Information.

Cell Isolation, Adoptive Transfer, and Immunization

Preparation of B cells and CD4$^+$ T cells are described in the Supplemental Information. In most experiments 1 to 5 × 10^5 Ag-specific B and T cells and 1 to 3 × 10^7 polyclonal B cells were transferred intravenously. In the experiment in Figure S5D, mice received 1 × 10^6 MD4 B cells of each genotype and 2 × 10^6 OT-II T cells. The mice were then immunized s.c. in the footpad, the base of the tail, the flank, and the scruff with 15 μg of OVA (Sigma-Aldrich), NP(13)-OVA (Bioresearch Technologies), or HEL-OVA mixed in alum (Thermo) or complete Freund's adjuvant (CFA, Sigma-Aldrich) per site unless otherwise indicated. For inducing thymus-independent Ab responses, NP(28)-Ficoll (Bioresearch Technologies) was i.p. injected.

Flow Cytometry and Cell Sorting

Cells were resuspended in PBS containing 2% FBS, 2 mM EDTA, and 0.05% NaN_3, stained with Abs, and analyzed on FACSCanto II (BD Biosciences). LN cells magnetically depleted of non-B cells or non-CD4$^+$ cells were sorted by FACSAria (BD Biosciences). The other information including those on the Abs and DNA content analysis are described in the Supplemental Information. Data were analyzed with FlowJo software (Tree Star, Inc.).

Immunofluorescence Microscopy

LNs were placed in Tissue-Tek OCT compound (Sakura) and "snap-frozen" in dry ice and ethanol. Cryostat sections (8 μm in thickness) were affixed to MAS-GP-coated slides (Matsunami Glass) and fixed in cold acetone for 10 min. The reagents used for staining LN sections are described in the Supplemental Information. Images were acquired on an epifluorescence microscope BZ-9000 (Keyence).

Two-Photon Microscopy and Image Analysis

Explanted LNs were prepared for imaging as previously described (Allen et al., 2007b). Imaging was performed with the TCS SP5 upright microscope (Leica Microsystems) equipped with the Leica 20×/1.00 NA water immersion objective or a BX61/FV1000 upright microscope (Olympus) equipped with an Olympus 20×/0.95 NA water immersion objective. Multiphoton excitation was provided by a Mai Tai HP Ti:Sapphire laser (Spectra Physics) tuned to 900 nm. The other information on the microscopes and image analysis are in the Supplemental Information.

Microarray Analysis, Quantitative RT-PCR, ELISA, Immunoblotting, and Statistical Analysis

Procedures for these analyses are described in the Supplemental Information.

ACCESSION NUMBERS

All microarray data are available in the Gene Expression Omnibus (GEO) database (http://www.ncbi.nlm.nih.gov/gds) under the accession number GSE24574.

SUPPLEMENTAL INFORMATION

Supplemental Information includes seven figures, one table, Supplemental Experimental Procedures, and five movies and can be found with this article online at doi:10.1016/j.immuni.2011.03.025.

ACKNOWLEDGMENTS

We thank J. Cyster, Y. Aiba, K. Kometani, D. Baumjohann, M. Ansel, and S. Fagarasan for discussion, N. Takahashi, E. Mori, M. Kurosaki, and the core facilities at RIKEN, RCAI for the technical assistance, M. Matsuda, S. Kiyonaka, Y. Wakabayashi, and T. Saito for help on setting up the microscopes. M.K. is a RIKEN Special Postdoctoral Researcher, and S.M. is a RIKEN Junior Research Associate. This work was supported by the Ministry of Education, Culture, Sports, Science and Technology of Japan (M.K., Y.M., T.K., and T.O.), the Uehara Memorial Foundation (T.O.), the Sumitomo Foundation (T.O.), and the Mochida Memorial Foundation for Medical and Pharmaceutical Research (T.O.).

Received: October 18, 2010
Revised: February 4, 2011
Accepted: March 10, 2011
Published online: June 2, 2011

REFERENCES

Allen, C.D., Ansel, K.M., Low, C., Lesley, R., Tamamura, H., Fujii, N., and Cyster, J.G. (2004). Germinal center dark and light zone organization is mediated by CXCR4 and CXCR5. Nat. Immunol. *5*, 943–952.

Allen, C.D., Okada, T., and Cyster, J.G. (2007a). Germinal-center organization and cellular dynamics. Immunity *27*, 190–202.

Allen, C.D., Okada, T., Tang, H.L., and Cyster, J.G. (2007b). Imaging of germinal center selection events during affinity maturation. Science *315*, 528–531.

Basso, K., and Dalla-Favera, R. (2010). BCL6: Master regulator of the germinal center reaction and key oncogene in B cell lymphomagenesis. Adv. Immunol. *105*, 193–210.

Bauquet, A.T., Jin, H., Paterson, A.M., Mitsdoerffer, M., Ho, I.C., Sharpe, A.H., and Kuchroo, V.K. (2009). The costimulatory molecule ICOS regulates the expression of c-Maf and IL-21 in the development of follicular T helper cells and TH-17 cells. Nat. Immunol. *10*, 167–175.

Cannons, J.L., Qi, H., Lu, K.T., Dutta, M., Gomez-Rodriguez, J., Cheng, J., Wakeland, E.K., Germain, R.N., and Schwartzberg, P.L. (2010). Optimal germinal center responses require a multistage T cell:B cell adhesion process involving integrins, SLAM-associated protein, and CD84. Immunity *32*, 253–265.

Carlson, C.M., Endrizzi, B.T., Wu, J., Ding, X., Weinreich, M.A., Walsh, E.R., Wani, M.A., Lingrel, J.B., Hogquist, K.A., and Jameson, S.C. (2006). Kruppel-like factor 2 regulates thymocyte and T-cell migration. Nature *442*, 299–302.

Chan, T.D., Gardam, S., Gatto, D., Turner, V.M., Silke, J., and Brink, R. (2010). In vivo control of B-cell survival and antigen-specific B-cell responses. Immunol. Rev. *237*, 90–103.

Crotty, S., Johnston, R.J., and Schoenberger, S.P. (2010). Effectors and memories: Bcl-6 and Blimp-1 in T and B lymphocyte differentiation. Nat. Immunol. *11*, 114–120.

Cyster, J.G. (2005). Chemokines, sphingosine-1-phosphate, and cell migration in secondary lymphoid organs. Annu. Rev. Immunol. *23*, 127–159.

Deenick, E.K., Chan, A., Ma, C.S., Gatto, D., Schwartzberg, P.L., Brink, R., and Tangye, S.G. (2010). Follicular helper T cell differentiation requires continuous antigen presentation that is independent of unique B cell signaling. Immunity *33*, 241–253.

Dent, A.L., Shaffer, A.L., Yu, X., Allman, D., and Staudt, L.M. (1997). Control of inflammation, cytokine expression, and germinal center formation by BCL-6. Science *276*, 589–592.

Fazilleau, N., Eisenbraun, M.D., Malherbe, L., Ebright, J.N., Pogue-Caley, R.R., McHeyzer-Williams, L.J., and McHeyzer-Williams, M.G. (2007). Lymphoid reservoirs of antigen-specific memory T helper cells. Nat. Immunol. *8*, 753–761.

Förster, R., Emrich, T., Kremmer, E., and Lipp, M. (1994). Expression of the G-protein—coupled receptor BLR1 defines mature, recirculating B cells and a subset of T-helper memory cells. Blood *84*, 830–840.

Fukuda, T., Yoshida, T., Okada, S., Hatano, M., Miki, T., Ishibashi, K., Okabe, S., Koseki, H., Hirosawa, S., Taniguchi, M., et al. (1997). Disruption of the Bcl6 gene results in an impaired germinal center formation. J. Exp. Med. *186*, 439–448.

Gatto, D., Paus, D., Basten, A., Mackay, C.R., and Brink, R. (2009). Guidance of B cells by the orphan G protein-coupled receptor EBI2 shapes humoral immune responses. Immunity *31*, 259–269.

Good-Jacobson, K.L., Szumilas, C.G., Chen, L., Sharpe, A.H., Tomayko, M.M., and Shlomchik, M.J. (2010). PD-1 regulates germinal center B cell survival and the formation and affinity of long-lived plasma cells. Nat. Immunol. *11*, 535–542.

Haynes, N.M., Allen, C.D., Lesley, R., Ansel, K.M., Killeen, N., and Cyster, J.G. (2007). Role of CXCR5 and CCR7 in follicular Th cell positioning and appearance of a programmed cell death gene-1high germinal center-associated subpopulation. J. Immunol. *179*, 5099–5108.

Hsu, H.C., Yang, P., Wang, J., Wu, Q., Myers, R., Chen, J., Yi, J., Guentert, T., Tousson, A., Stanus, A.L., et al. (2008). Interleukin 17-producing T helper cells and interleukin 17 orchestrate autoreactive germinal center development in autoimmune BXD2 mice. Nat. Immunol. *9*, 166–175.

Johnston, R.J., Poholek, A.C., DiToro, D., Yusuf, I., Eto, D., Barnett, B., Dent, A.L., Craft, J., and Crotty, S. (2009). Bcl6 and Blimp-1 are reciprocal and antagonistic regulators of T follicular helper cell differentiation. Science *325*, 1006–1010.

Klein, U., and Dalla-Favera, R. (2008). Germinal centres: Role in B-cell physiology and malignancy. Nat. Rev. Immunol. *8*, 22–33.

Kurosaki, T., Aiba, Y., Kometani, K., Moriyama, S., and Takahashi, Y. (2010). Unique properties of memory B cells of different isotypes. Immunol. Rev. *237*, 104–116.

Linterman, M.A., and Vinuesa, C.G. (2010). Signals that influence T follicular helper cell differentiation and function. Semin. Immunopathol. *32*, 183–196.

MacLennan, I.C. (1994). Germinal centers. Annu. Rev. Immunol. *12*, 117–139.

Martins, G., and Calame, K. (2008). Regulation and functions of Blimp-1 in T and B lymphocytes. Annu. Rev. Immunol. *26*, 133–169.

Morita, R., Schmitt, N., Bentebibel, S.E., Ranganathan, R., Bourdery, L., Zurawski, G., Foucat, E., Dullaers, M., Oh, S., Sabzghabaei, N., et al. (2011). Human blood CXCR5(+)CD4(+) T cells are counterparts of T follicular cells and contain specific subsets that differentially support antibody secretion. Immunity *34*, 108–121.

Nurieva, R.I., Chung, Y., Martinez, G.J., Yang, X.O., Tanaka, S., Matskevitch, T.D., Wang, Y.H., and Dong, C. (2009). Bcl6 mediates the development of T follicular helper cells. Science *325*, 1001–1005.

Nutt, S.L., Fairfax, K.A., and Kallies, A. (2007). BLIMP1 guides the fate of effector B and T cells. Nat. Rev. Immunol. *7*, 923–927.

Okada, T., Miller, M.J., Parker, I., Krummel, M.F., Neighbors, M., Hartley, S.B., O'Garra, A., Cahalan, M.D., and Cyster, J.G. (2005). Antigen-engaged B cells undergo chemotaxis toward the T zone and form motile conjugates with helper T cells. PLoS Biol. *3*, e150.

Pereira, J.P., Kelly, L.M., Xu, Y., and Cyster, J.G. (2009). EBI2 mediates B cell segregation between the outer and centre follicle. Nature *460*, 1122–1126.

Pereira, J.P., Kelly, L.M., and Cyster, J.G. (2010). Finding the right niche: B-cell migration in the early phases of T-dependent antibody responses. Int. Immunol. *22*, 413–419.

Poholek, A.C., Hansen, K., Hernandez, S.G., Eto, D., Chandele, A., Weinstein, J.S., Dong, X., Odegard, J.M., Kaech, S.M., Dent, A.L., et al. (2010). In vivo regulation of Bcl6 and T follicular helper cell development. J. Immunol. *185*, 313–326.

Qi, H., Cannons, J.L., Klauschen, F., Schwartzberg, P.L., and Germain, R.N. (2008). SAP-controlled T-B cell interactions underlie germinal centre formation. Nature *455*, 764–769.

Reinhardt, R.L., Liang, H.E., and Locksley, R.M. (2009). Cytokine-secreting follicular T cells shape the antibody repertoire. Nat. Immunol. *10*, 385–393.

Schwickert, T.A., Alabyev, B., Manser, T., and Nussenzweig, M.C. (2009). Germinal center reutilization by newly activated B cells. J. Exp. Med. *206*, 2907–2914.

Shaffer, A.L., Rosenwald, A., Hurt, E.M., Giltnane, J.M., Lam, L.T., Pickeral, O.K., and Staudt, L.M. (2001). Signatures of the immune response. Immunity *15*, 375–385.

Shih, T.A., Roederer, M., and Nussenzweig, M.C. (2002). Role of antigen receptor affinity in T cell-independent antibody responses in vivo. Nat. Immunol. *3*, 399–406.

Simpson, N., Gatenby, P.A., Wilson, A., Malik, S., Fulcher, D.A., Tangye, S.G., Manku, H., Vyse, T.J., Roncador, G., Huttley, G.A., et al. (2010). Expansion of circulating T cells resembling follicular helper T cells is a fixed phenotype that identifies a subset of severe systemic lupus erythematosus. Arthritis Rheum. *62*, 234–244.

Tokoyoda, K., Zehentmeier, S., Hegazy, A.N., Albrecht, I., Grün, J.R., Löhning, M., and Radbruch, A. (2009). Professional memory CD4+ T lymphocytes preferentially reside and rest in the bone marrow. Immunity *30*, 721–730.

Victora, G.D., Schwickert, T.A., Fooksman, D.R., Kamphorst, A.O., Meyer-Hermann, M., Dustin, M.L., and Nussenzweig, M.C. (2010). Germinal center dynamics revealed by multiphoton microscopy with a photoactivatable fluorescent reporter. Cell *143*, 592–605.

Vinuesa, C.G., Sanz, I., and Cook, M.C. (2009). Dysregulation of germinal centres in autoimmune disease. Nat. Rev. Immunol. *9*, 845–857.

Vinuesa, C.G., Linterman, M.A., Goodnow, C.C., and Randall, K.L. (2010). T cells and follicular dendritic cells in germinal center B-cell formation and selection. Immunol. Rev. *237*, 72–89.

Ye, B.H., Cattoretti, G., Shen, Q., Zhang, J., Hawe, N., de Waard, R., Leung, C., Nouri-Shirazi, M., Orazi, A., Chaganti, R.S., et al. (1997). The BCL-6 proto-oncogene controls germinal-centre formation and Th2-type inflammation. Nat. Genet. *16*, 161–170.

Yu, D., Rao, S., Tsai, L.M., Lee, S.K., He, Y., Sutcliffe, E.L., Srivastava, M., Linterman, M., Zheng, L., Simpson, N., et al. (2009). The transcriptional repressor Bcl-6 directs T follicular helper cell lineage commitment. Immunity *31*, 457–468.